Dynamically Avoiding Amorphous Obstacles with Topological Manifold Learning and Deep Autoencoding

Apan Dastider and Mingjie Lin

Abstract—To achieve conflict-free human-machine collaborations, robotic agents need to skillfully avoid continuously moving obstacles while achieving collective objectives. Sometimes, these obstacles can even change their 3D shapes and forms simultaneously, hence being "amorphous". To this end, this paper formulates the problem of Dynamic Amorphous Obstacle Avoidance (DAO-A), where a robotic arm can dexterously avoid dynamically generated obstacles that constantly change their trajectories and their 3D forms.

Specifically, we introduce a novel control strategy for robotic arms that leverages both topological manifold learning and latest deep learning advancements. We test our learning framework, using a 7-DoF robotic manipulator, in both simulation and physical experiments, where the robot satisfactorily learns and synthesizes realistic skills avoiding previously-unseen obstacles, while generating novel movements to achieve pre-defined motion objectives. Most notably, our learned methodology, once finalized, for a given robotic manipulator, can avoid any number of 3D obstacles with arbitrary and unseen moving trajectories, therefore it is universal, versatile, and completely reusable.

Index Terms—Obstacle Avoidance, Deep Learning, Manifold Learning, Graph Traversal

I. Introduction

With the advent of fourth industry revolution, safe humanrobot collaboration becomes increasingly more essential in most manufacturing facilities [1], [2]. While in obstacle-free environments, the motion planning of a robotic arm can be readily solved by off-the-shelf algorithms, it is significantly more involved in unstructured environments when (static and dynamic) obstacles occupy the robot workspace [3]. Moreover, if the robot arm aims at achieving variable or even dynamically-changing motion objectives, the difficulty level of active obstacle avoidance by a robotic arm exacerbates. Previously, solving obstacle avoidance problems mostly relied on dynamical-system-based approaches [4], [5] that effectively model motion dynamics, often augmented with sophisticated probabilistic methods [6] that account for data variability and model uncertainty. Very recently, prompted by the astronomical advances in DNN (Deep Neural Network), many researchers have attempted to tackle obstacle avoidance from a deep learning perspective, where the complex motion dynamics between a robotic arm and its obstacles are captured through applying various reinforcement learning methodologies [7]. Despite all these advancements, numerous challenges remain formidable: generalized methodology for different robotic arms and different objectives, unified framework of solving obstacle avoidance, and handling multiple dynamically moving and morphing 3D obstacles, among others.

In this paper, in order to address several of the aforementioned challenges, we present an innovative approach from a topological manifold perspective for robotic motion planning to avoid obstacles, as illustrated in Fig. 1. Unlike

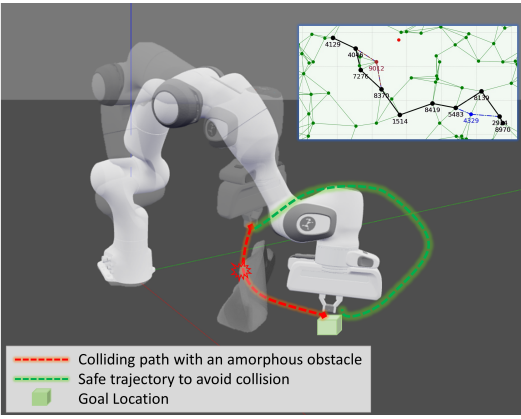


Fig. 1: A 7-DoF robotic manipulator needs to reach a target while avoiding a dynamically moving and changing obstacle. From accumulated dataset we learn a variational autoencoder that spans a random topological manifold. The motion control of this manipulator is computed by dynamically traversing a 2D graph generated by manifold learning. The forward and backward mappings between high-dimensional robotic pose space and low-dimensional manifold space are computed by an autoencoder implemented with two independent deep neural networks (DNNs).

previous works [4], [6]–[8], where complex system dynamics modelling is essential or computation of multiple networks on latent space is necessary, we leverage a unique manifold learning-based framework that emphasizes on dynamically avoiding amorphous/shape-changing obstacles while achieving one or multiple objectives. Specifically, as depicted in Fig. 2:

- We first learn a 2D manifold space that captures the whole system dynamics between a whole-body robotic arm and an any-location point obstacle while reaching for a fixed objective.
- Subsequently, we synthesize a single topological graph with nearest-neighborhood principle and employ standard graph traversing algorithms to perform efficient motion planning for our robotic arm.
- In addition, we construct two pairing deep neural networks (autoencoder and autodecoder) to translate between full-pose joint-space trajectories and routed paths on our learned manifold surface.
- Finally, we develop a fail-safe algorithm to adaptively adjust our robotic motion planning on the fly to compensate the inevitable inaccuracy due to manifold learning as well as generalize our algorithm to tackle any dynamic obstacles by redefining via-points of graph traversing.

The most distinctive advantage of our methodology is its generalization capability to handle any number of dynamic obstacle with arbitrary shapes once its fundamental underlying manifold surface is learned. We illustrate our approach with a 7-DoF robotic manipulator avoiding dynamic obstacles with arbitrary shapes. We have conducted extensive experiments to illustrate how our approach learns and reproduces realistic robot skills featuring complex motion patterns and obstacle avoidance. Moreover, we demonstrate how our approach can seamlessly handle unseen new obstacles that not only move but also change their number and locations without incurring any new learning efforts. In summary, we contribute a new view on robotic motion planning that take advantage of classic manifold learning and newly-developed deep learning. We show how dynamic obstacle avoidance problem with arbitrary settings can be readily reduced into solving a basic point obstacle avoidance problem.

II. RELATED WORKS

Recently, attention has been given to formulate latent space representation and topological manifold learning for smoother robotic motion planning and obstacle avoidance. For instance, [9] developed a Riemannian submanifold in $\mathbb{R}^3 \times \mathcal{S}^3$ space and expoited geodesics path over the learned sub-manifold for robotic motion generation. [9] also introduced obstacle avoidance scheme through re-modifying the ambient metrics in the latent space. Besides, [8] learned a latent space network through auto-encoding, developed a sampling-based motion planning over such networks and obstacle avoidance by traversing another collision checking network in addition to motion planning network. Moreover, [10] proposed an optimal tracking control by recurrent knowledge based heuristics and obstacle avoidance solution through recording the proximal distance between 3D meshes. In general, recent works have tried to introduce manifold representation for learning various robotic skills in lowdimensional space. On the contrary, we presented here a more scalable and simpler solution to shape changing obstacle avoidance problems in real-time through traversing a single and unique densely-connected 2D network of manifold representation of high-dimensional robotic state space without additional computational overheads.

III. PROBLEM FORMULATION

Motion control of a given robotic manipulator calculates a specified joint-space trajectory, typically defined with a function of its joint angles, in order to reach a desired position of its end effector. Mathematically, let us consider a k-DOF robotic manipulator operating in an n-dimensional task space (n=3 for spatial position). The forward kinematic mapping is a surjective function of the joint-space coordinates

$$\mathbf{x}(t) = f(\theta(t)),\tag{1}$$

where $\mathbf{x}(t) \in \mathbb{R}^n$ and $\theta(t) \in \mathbb{R}^k$ are the task-space and joint-space coordinates, respectively. Note that k > n for a redundant manipulator. As a nonlinear vector-valued function, the forward kinematic mapping $f(\cdot)$ is straightforward to formulate using the mechanical design and Denavit-Hartenberg parameters for a given manipulator. However, the task for a manipulator is usually specified in the Cartesian task space instead of the joint space. Therefore, computing the inverse mapping, i.e., mapping from the task space to the joint space, usually is more important. Using Equation 1, we can define an inverse kinematics model as

$$\theta(\mathbf{t}) = f^{-1}(\mathbf{x}(t)),\tag{2}$$

where $f^{-1}(\cdot)$ denotes the inverse kinematic mapping. For a given target, our goal is to solve the above equation for the value of $\theta(t)$ in the joint space. However, for a redundant manipulator, the forward kinematic mapping $f(\cdot)$ is surjective only and not one-to-one, i.e., there exist infinite solutions $\theta(t)$ in the joint space. To resolve the redundancy, i.e., calculate an optimal joint-space trajectory out of infinitely many possible trajectories, we model the tracking control as an optimization problem that minimizes a pre-defined cost function, i.e.,

$$\theta^*(\mathbf{t}) = \operatorname*{arg\,min}_{\theta(\mathbf{t}) = f^{-1}(\mathbf{x}(t))} \mathcal{C}(\theta(t), \mathbf{x}(t)), \tag{3}$$

where $\mathcal{C}(.)$ is user-defined cost function. Unfortunately, the solution to the above optimization problem does not guarantee that the manipulator does not collide with an obstacle. In this work, we formulate the problem of obstacle avoidance as the problem of maximizing the minimum distance between the links of the manipulator and the obstacle. To incorporate this consideration into our control framework, we formulate an objective function that penalizes the angles in joint space that bring the robot close to the obstacle. Specifically, the obstacle avoidance optimization problem is defined as the same as Equation 3 except that the cost function $\mathcal{C}(.)$ is defined as

$$C(\theta(t), \mathbf{x}(t), \mathbf{o}(t)) = \frac{1}{[\min_{i \in \{1, 2, \dots, k\}} d_i(\mathbf{o}(t), \theta(t))]^{\beta}}, \quad (4)$$

where $\mathbf{o}(t)$ is a dynamically changing obstacle and β is a hyperparameter. Overall, this cost function of a reciprocal relationship ensures that the increasing distance between all joints and obstacles will significantly increase the overall cost. Here, the distance $d_i(\mathbf{o}(t), \theta(t))$ is computed by the well-known Gilbert-Johnson-Keerthi (GJK) algorithm [10], [11] given the 3D collision meshes of our 7-DoF robotic manipulator at particular joint-space configuration $\theta(t)$ and the 3D geometrical mesh of the obstacle $\mathbf{o}(t)$.

IV. PROPOSED METHODOLOGY

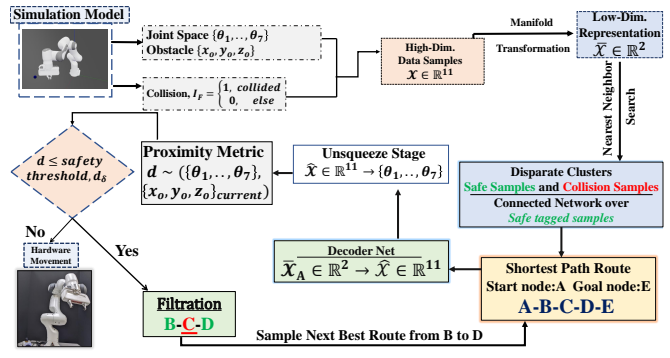


Fig. 2: Algorithmic block digram of our overall methodology.

Figure 2 depicts the overall structure of our proposed methodology. It consists of three major algorithm modules: 1) topological manifold learning, which transforms high-dimensional robotic poses into low-dimensional 2D data points in order to facilitate robotic path planning and obstacle avoidance, 2) variational autoencoding/decoding, which bridges between high-dimensional robotic poses and low-dimensional manifold spaces, and 3) graph construction and traversing, which performs robotic control and obstacle

avoidance by traversing and rerouting a 2D fully-connect graph efficiently.

Algorithm Block 1: Topological Manifold Learning

Manifold learning is a well-known mathematical framework for investigating the geometrical structure of datasets of high-dimensional spaces. In this paper, we consider the high-dimensional space defined by $[\theta_0, \dots, \theta_6; [x, y, z]_o; \mathbb{I}_F]$, where θ_i s determine the exact full joint-space pose of a robotic arm, and $[x,y,z]_o$ defines the location of a point obstacle. \mathbb{I}_F is a boolean collision flag. Our crucial insight is that the geometrical structure of our considered highdimensional space incorporates the complex system dynamic between any full pose of a chosen robotic arm and a point obstacle at arbitrary location. In order to fully extract and leverage the embedding power of our learned manifold, we perform a dimension reduction following techniques of a well-known isometric embedding [12] from highdimensional robotic space to the low-dimensional manifold space that can be more readily utilized for robotic motion planning. It is important to note that all these dimension reductions are done under the condition that the metric tensor is preserved between these two spaces.

Algorithm Block 2: Variational Autoencoding/Decoding

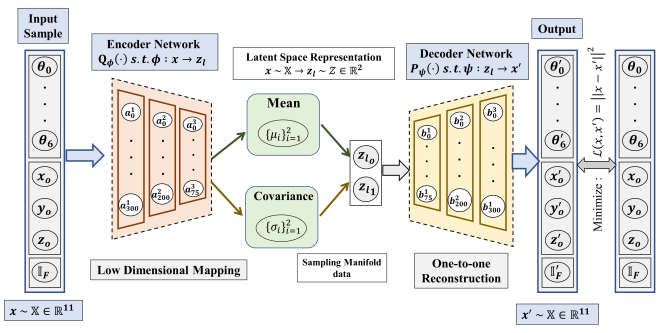


Fig. 3: Schematic of Variational autoencoder used for Manifold Learning.

To facilitate our manifold-based robotic motion planning, we need to seamlessly transform between high-dimensional robotic space, \mathcal{R} and low-dimensional manifold space, \mathcal{Z} . For this, we use a well-established deep learning technique: variational autoencoder (VAE) [13]. Conceptually, an autoencoder consists of both an encoder and a decoder. In fact, autoencoders are typically forced to reconstruct the input approximately, preserving only the most relevant aspects of the data in the copy. In our study, we implemented autoencoders as deep neural networks in order to perform dimensionality reduction and reconstruction of samples. Specifically, as conceptually depicted in Fig. 3, our autoencoder is implemented as a feedforward, non-recurrent neural network employing an input layer and an output layer connected by multiple hidden layers. The output layer has the same number of nodes (neurons) as the input layer. The purpose of our autoencoder is to reconstruct its inputs (minimizing the difference between the input and the output) instead of predicting a target value X' given inputs X.

Our autoencoder consisted of two parts, the encoder and the decoder, which can be defined as transformation functions Q_{ϕ} and P_{ψ} , such that: $\phi: \mathcal{X} \to z_l$ and $\psi: z_l \to \mathcal{X}'$ and $\phi, \psi = \arg\min \|\mathcal{X} - (\psi \circ \phi)\mathcal{X}\|^2$. This two-way mapping can be considered as one-to-one and onto function

between input and output layers. Autoencoders were trained to minimize reconstruction errors (such as squared errors), often referred to as the "loss", $\mathcal{L}(\mathbf{x},\mathbf{x}') = \|\mathbf{x} - \mathbf{x}'\|^2$, where \mathbf{x} is usually averaged over the training set. Our autoencoder is trained through backpropagation of the error. Conceptually, the feature space z_l of our autoencoder is the low-dimension manifold representations produced by manifold learning, therefore having lower dimensionality than the input space \mathcal{X} , which, in our study, is the pose of our 7-DoF robotic manipulator with object position and collision flag. As such, the feature matrix $Q_{\phi}(x)$ after manifold learning can be regarded as a compressed representation of the input x.

Algorithm Block 3: Graph Construction and Traversing

Graph-based robotic motion planning has been well established [14], however mostly applied in the arena of mobile robots navigating in complex environments [15], [16]. In this work, the graph we have constructed encodes the complex system dynamic between robotic manipulator and its obstacle through a topological manifold space. In our study, we choose to use \mathbb{R}^2 space for our low-dimensional manifold space to simplify our graph data structure and its traversing. Specifically, after our manifold space is created, we will have a set of vertices labeled either as "collision" or "collision free/safe" samples. During our robotic arm motion planning, we will perform shortest-distance routing using the wellknown Dijkstra's algorithm with only the green vertices ('collision-free/safe"). The graph internal data structures of our 2D graph are based on an adjacency list representation and implemented using Python dictionary data structures. Furthermore, the graph adjacency structure is implemented as a Python dictionary of dictionaries; the outer dictionary is keyed by nodes to values that are themselves dictionaries keyed by neighboring node to the edge attributes associated with that edge. This "dict-of-dicts" structure allows fast addition, deletion, and lookup of nodes and neighbors in large graphs. All of our functions manipulate graph-like objects solely via predefined API methods and not by acting directly on the data structure. Our software code is largely based on the open-source NetworkX package [17].

V. SYSTEM OVERVIEW

A. Experimental Platform and Simulation Setup

For real hardware demonstrations, we considered here a 7-DoF Franka Emika Panda robot arm, that is mounted on table-top which served as a concise workspace for completing all experiments as shown in Fig. 10. Our adaptive trajectory planning algorithm runs on a Lambda QUAD GPU workstation equipped with Intel Core-i9-9820X processor through straightforward Python implementation. Besides, we utilized here a Intel RealSense Depth Camera D435i for tracking the dynamic obstacle and extracting the depth information to obtain the position in 3D camera coordinate frame. Through applying the mathematical formulation of conventional hand-to-eye calibration, the $[x, y, z]_o$ information in camera reference frame has been transported to the robot coordinate system. These feedback of depth sensors were exploited by our algorithm to re-route the trajectory for avoiding any shaped obstacles in real-world scenarios. Basically, we applied here the GJK algorithm to compute the

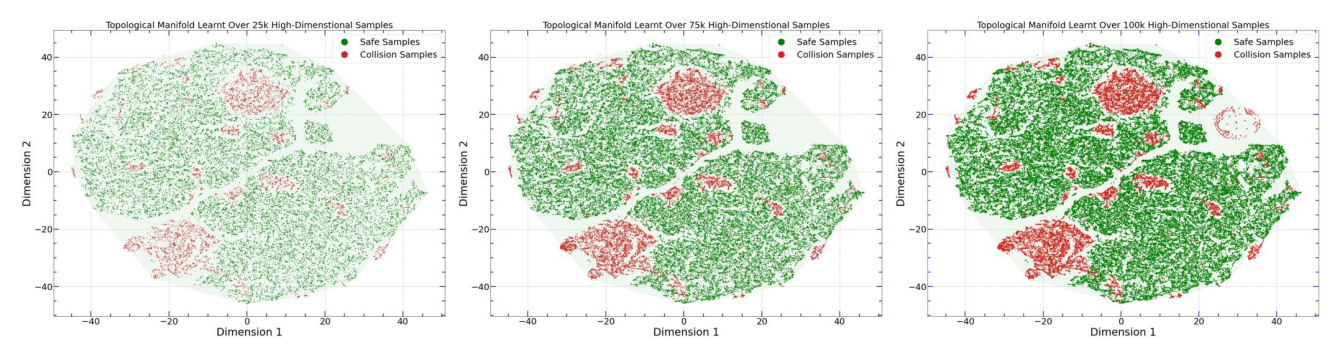


Fig. 4: Structure of Topological Manifold with varying number of input samples. (a) contains only 10k samples, (b) contains 25k samples, (c) shows manifold for full 100k samples collected

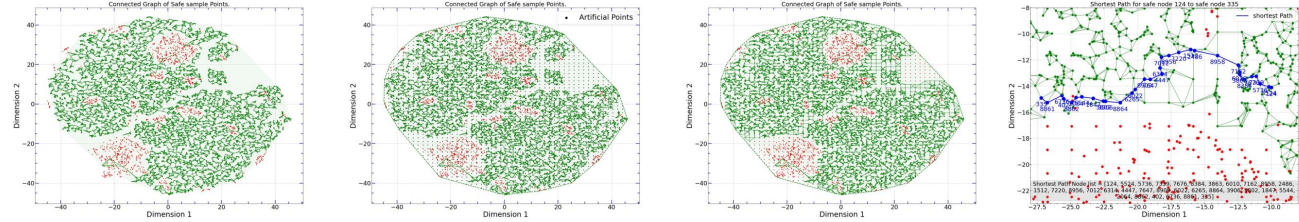


Fig. 5: (a) Connected Network over 10k Manifold Points (To have a clear visual, we plotted the network with 10k points. All planning were completed with full dataset), (b)-(c) Uniformly Sampled Points for a densely Connected Network, (d) Shortest Path Routing by Dijkstra's algorithm

distance between the 3D geometry of the obstacle and the collision meshes of robot links to safely route to the target location. On the other hand, to safely accumulate dataset and rigorously validate our approach, we replicated the exact model of Franka Emika Panda Arm inside Robotics Toolbox (RTB) for Python [18] which has been very recently released for robotics research. For establishing the low-latency and low-noise communication protocol to ensure data processing and parallel execution among simulation environments and real hardware, we encapsulated the full framework inside the Robot Operating System (ROS) ecosystem through utilizing libfranka and Franka ROS.

B. Experimental Procedures and Learning Variables

We gathered here high-dimensional data samples from robot's workspace which has been transformed into a latent space representation for creating the topological manifold. Each high data sample contains 11 numerical variables-7 joint angles $\{\theta_i\}_{i=0,\dots,6}$, position of point obstacle in \mathbb{R}^3 space and binary collision flag, $\mathbb{I}_{\mathbb{F}}$. The robot arm is controlled by sending Θ_i – a vector of 7 joint angles. The simulated environment was primarily used for dataset accumulation task and initial learning purposes. We opted out of the method Learning from Demonstrations(LfD) to avoid any biases and bring maximum variance in the dataset through randomly manipulating arm for very large number of epochs. This dataset contains in total 100k samples of joint values against different positions of point obstacles with respective collision flags. We focused more to collect adequate collision samples to have a safer elementary trajectory required. When the algorithm and manifold learning converged, the test experiments were conducted against varying occlusions created by geometrically different 3D objects in real hardware setup for real-time and scalable applications. Our VAE architecture is implemented on Pytorch [19]. The decoder and encoder network comprises on three layers with {300, 200, 75} neurons on each layer. The encoded latent space representation lies in \mathbb{R}^2 which greatly facilitates

creating graph embedding to plan optimal path from a start node to goal node.

VI. RESULTS ANALYSIS

Our experiments seek to investigate the following:

- 1) Can we learn a globally preserved manifold representation in \mathbb{R}^2 space for varying bins of samples differentiating the non-colliding and colliding samples?
- 2) Can our proposed approach assure that the robotic entity is firmly able to avoid geometrically varying and 3D amorphous obstacles?
- 3) Can we concurrently track the unseen perturbations through depth information and dynamically adjust the trajectory to reach the goal location?

A. Latent Space Representation and Optimum Routing

Each high-dimensional input sample contains the joint angle vector for moving arm, the 3D coordinate locations of the obstacle and a collision flag I_F . From this highdimensional representation, our VAE learns a topological manifold representation in \mathbb{R}^2 . As shown in Fig.4, the latent space manifold representation can be visually splitted into contrasting clusters of two binary level collision flag. On the next step, we constructed a connected graph over \mathbb{R}^2 space encompassing the safe samples in green color shown in Fig.5(a). By applying unsupervised K-Nearest Neighbor algorithm [20] for finding nearest family of vertices in the safe manifold space, we created here a connected graph network which accelerates any shortest path routing algorithm to traverse on transformed low-dimensional manifold sample. As shown in Fig.5(a), while creating connected graphs, disconnected sub-networks were created automatically inside the safe manifold as nearest neighboring algorithm only assists to create connected network at closest distance. This generation of sub-networks violates highly the notion of complete path routing from any random node to another random node on the fully connected network. To confirm a dense connection, we artificially sampled points in same \mathbb{R}^2 space as a grid mesh over the learnt \mathbb{R}^2 space. By

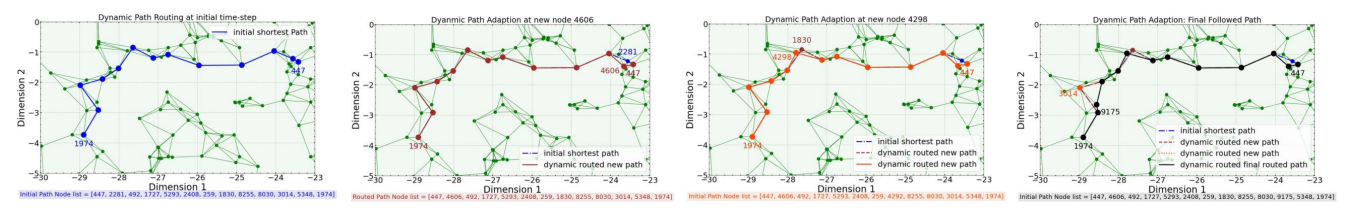


Fig. 6: Dynamic Path routing for avoiding collision: (a) Initial Sampled Path (b)-(c) Path Change for avoiding dynamic perturbations (c) Comparison of final followed path and initial path

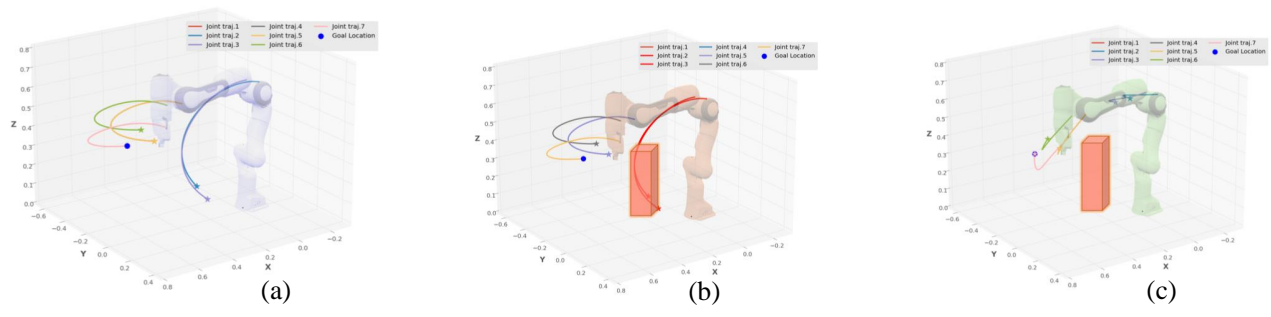


Fig. 7: Change of Joint Space trajectories for each joint when a random obstacle blocks the initial planned trajectory. In shaded colors of robot structure, respectively initial, colliding and safe planning has been depicted.

tuning the level of sparsity in creating the grid of artificial points, we can easily sample denser artificial points to create densely connected network. With our trained decoder part of VAE, we can stamp these artificial points as safe/colliding sample points which is shown in Fig.5(c). Here, it should be mentioned that Fig.5 is drawn over only 10k samples only to create a visibly clear image of connected network and sampled points. The overall learning happens with help of total collected and transformed low latent sample representation. Now, we obtained a densely connected network over all safe samples which guarantees that our elementary routed path can be presumed to be a safer trajectory. To sample the shortest path over the connected network, we have incorporated here a very well-known shortest path routing algorithm—Dijkstra's algorithm.

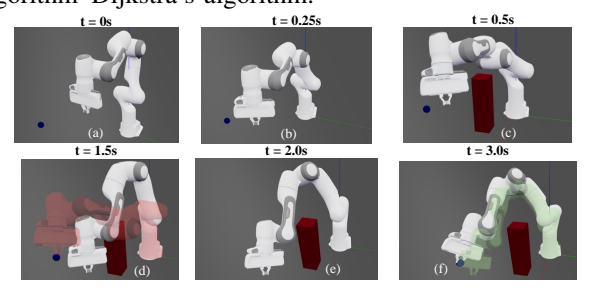


Fig. 8: (a) Initial pose, (b) Robot follows its initial path, (c) Obstacle appears at different time-step and robot stops it previous motion, (d) Robot revises its trajectory to avoid possible collision, in red shaded – collision when the trajectory planning *non-adaptive*, (e) (f) New trajectory while avoiding obstacle

B. Dynamic Obstacle Avoidance through Route Change

The principal target of our study is to propose a realtime dynamic obstacle avoidance method established on 2-D manifold representation and enable the robotic arm to concurrently revise its elementary planned trajectory to reach preset goal position within shortest possible time. Since, we have already constructed a densely connected networks of safe samples, and our artificial point sampling method guarantees at least one connecting path between any two random nodes, the algorithm can effortlessly perturb the initial route on real-time at any colliding node and form a new route by changing the intermediate node and edge connections. This dynamic interruption occurs when at any time-step a moving occlusion blocks the robot's movement following the initial trajectory. The adaptive robotic arm then receives a adversarial feedback of possible collision through distance measurement and adaptively reforms its initial path based on nearest neighbor network as shown in Fig.6. The algorithm guides the robotic arm to revise the shortest path by forming new intermediate vertices to vertices connections as depicted in Fig.6. Moreover, the decoder part of the VAE is employed to get joint poses for selected manifold points.

In Fig.7, we have showed in a 3D plot how the joint space configuration changed when a randomly placed obstacle against the initial trajectory blocked robot's safe movement and our method concurrently planned to reach the target position through a new trajectory path. From Fig.7(b), it is clear that if the robotic manipulator blindly follows the initial path, it will head to a possible catastrophe of collision which can damage both mechanical structure and surrounding. Besides, in Fig.8, we included the snapshots of robotic behavior inside the simulated environment. Initially, the robotic arm tried to reach the goal position following its sampled initial trajectory. But at a later timestep showed in Fig.8(c), a dynamically set obstacle blocked the robot motion. So, our proposed method would efficiently guide the robotic arm to re-route through a new trajectory. With the new planned trajectory, the robotic arm dodges the obstacle and moves around the red block to avoid a possible collision. In the last snapshot, we can finalize that the arm has reached the goal position smoothly and safely.

C. Handling Geometrically Varying Obstacles

Since the proposed approach leverages a densely connected network of transformed manifold representations and shortest routing algorithm, our proposed approach can be easily extended for avoiding probable collision with any shaped obstacles. In Fig.9, we attempted to graphically convey an idea on how the same adaptive routing successfully worked when the robot's initial motion was convoluted with

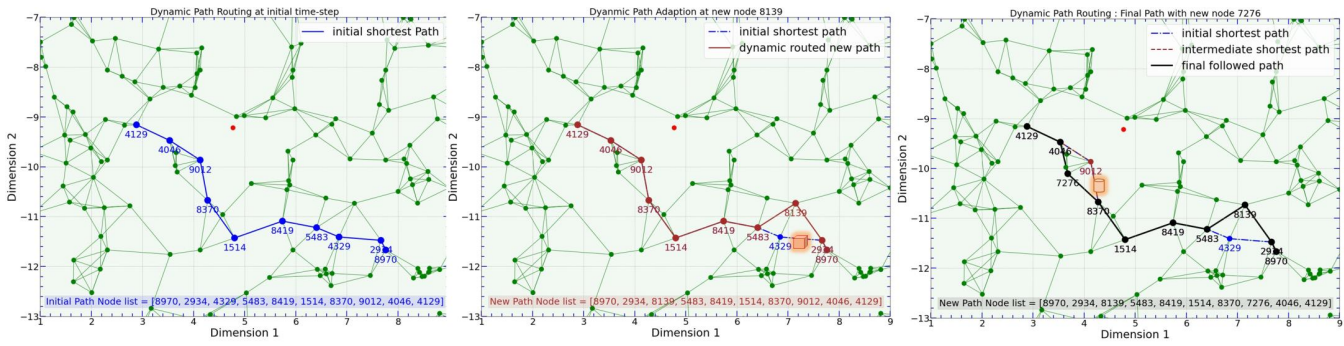


Fig. 9: Addressing the presence of any amorphous obstacles and avoiding collision through sampling new path from the connected networks

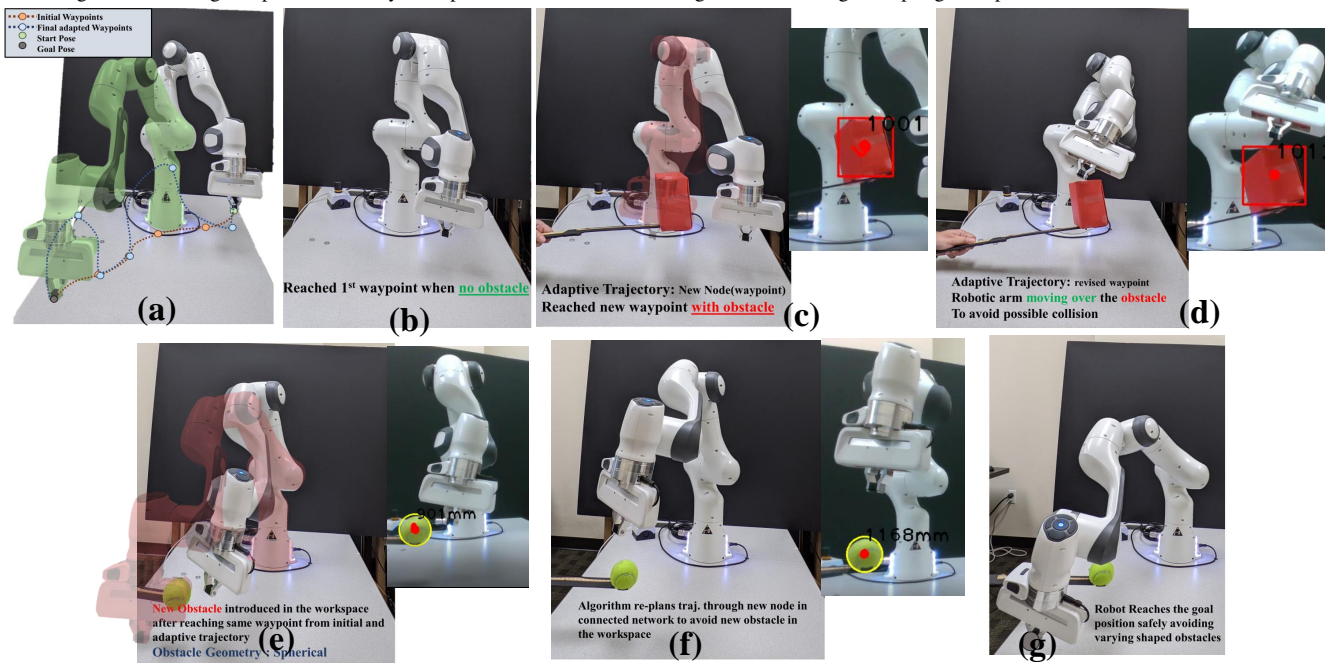


Fig. 10: (a) Comparison between initial waypoints and final waypoints, (c) Presence of obstacle, Depth Information extraction about pose of obstacle(cropped image) (d) Routing over the obstacle to avoid collision, (e) Reached next waypoint while again perturbed by different shaped-spherical obstacle, pose of new obstacles extracted through depth information, (f) algorithm enables the arm to dodge the collision, (g) Robot arm reaches its goal position successfully

presence of different shaped obstacles. For instance, the routing performed successfully even when the 3D shape of obstacles varied between a cuboid mesh and cylindrical mesh. Thus, our proposed method greatly generalizes for avoiding any shaped dynamic obstacle which makes it plausible to introduce our obstacle avoidance mechanism in human-robot collaborative work. Inside the RTB simulated environment, integrated high functionality API can be effortlessly used to track the proximal distance among 3D meshes. This API has been modified with the GJK algorithm for calculating the proximity among 3D meshes. This functionality produced a feedback to the controller when the robot's mechanical structure reaches very close to an obstacle. When this proximity value breaks the threshold safety metric, the robot controller is triggered to halt its current trajectory motion and revise its intermediate node connectivity to reach the preset goal position. On hardware setup, we localized obstacles in consecutive frames by applying color filtering through HSV color model and tracked the spatial positions of random obstacles through depth information extracted from Realsense depth camera. After successful extraction of depth values, we transported the 3D coordinate values with safety barrier around the obstacles to the learning controller and the

ontroller evaluated whether proximity distance violates the safety threshold metric. If the condition is suddenly violated, the algorithm replans for a new shortest and safest path to reach the goal position. In Fig.10, we have added snapshots from real hardware operation. In red shaded figure, we also depicted the probable collision would occur without the presence of dynamic adaption on real time. Here, we validated our experiments with varying size and different geometric objects. For both obstacles, our adaptive motion planning approach successfully avoided the dynamic obstacles which appear at different time-step of robot operation.

VII. CONCLUSION

Dynamically avoiding amorphous obstacles can be effectively tackled by combining three theoretical algorithm modules, namely topological manifold learning, variational autoencoding, and graph traversing and routing. Although each one of them is well studied, these algorithms, joined together, can solve the dynamic obstacle problems systematically and uniformly. In particular, for a given robotic manipulator, once our learned methodology is finalized, it can avoid any number of 3D obstacles with arbitrary and unseen moving trajectories, which renders our proposed methodology universal, versatile, and completely reusable.

REFERENCES

- M. A. Goodrich and A. C. Schultz, "Human-robot interaction: A survey," Foundations and Trends in Human-Computer Interaction, vol. 1, no. 3, pp. 203–275, 2007.
- [2] P. S. Schmitt, F. Witnshofer, K. M. Wurm, G. V. Wichert, and W. Burgard, "Modeling and planning manipulation in dynamic environments," *Proceedings - IEEE International Conference on Robotics* and Automation, vol. 2019-May, pp. 176–182, 2019.
- [3] D. Falanga, K. Kleber, and D. Scaramuzza, "Dynamic obstacle avoidance for quadrotors with event cameras," *Science Robotics*, 2020.
- [4] S. Sundar and Z. Shiller, "Optimal obstacle avoidance based on the hamilton-jacobi-bellman equation," *IEEE Transactions on Robotics* and Automation, vol. 13, no. 2, pp. 305–310, 1997.
- [5] S. M. Khansari-Zadeh and A. Billard, "A dynamical system approach to realtime obstacle avoidance," *Autonomous Robots*, vol. 32, no. 4, pp. 433–454, 2012.
- [6] L. Blackmore, M. Ono, and B. C. Williams, "Chance-constrained optimal path planning with obstacles," *IEEE Transactions on Robotics*, vol. 27, no. 6, pp. 1080–1094, 2011.
- [7] A. Garg, H.-T. L. Chiang, S. Sugaya, A. Faust, and L. Tapia, "Comparison of deep reinforcement learning policies to formal methods for moving obstacle avoidance," IEEE/RSJ International Conference on Intelligent Robots and Systems (IROS), pp. 3534–3541, 2019. [Online]. Available: https://storage.googleapis.com/pub-tools-public-publication-data/pdf/ 67343108f477d3a599a3e9be2f7400000a296289.pdf
- [8] B. Ichter and M. Pavone, "Robot motion planning in learned latent spaces," *IEEE Robotics and Automation Letters*, vol. 4, no. 3, pp. 2407–2414, 2019.
- [9] H. B. Mohammadi, S. Hauberg, G. Arvanitidis, G. Neumann, and L. D. Rozo, "Learning riemannian manifolds for geodesic motion skills," in *Robotics: Science and Systems*, 2021. [Online]. Available: https://doi.org/10.15607/RSS.2021.XVII.082
- [10] A. H. Khan, S. Li, and X. Luo, "Obstacle Avoidance and Tracking Control of Redundant Robotic Manipulator: An RNN-Based Metaheuristic Approach," *IEEE Transactions on Industrial Informatics*, vol. 16, no. 7, pp. 4670–4680, 2020.
- [11] M. Lin and S. Gottschalk, "Collision detection between geometric models: A survey," Proc. of IMA conference on mathematics of Surfaces, pp. 1–20, 1998. [Online]. Available: http://users.soe.ucsc.edu/\$\sim\$pang/161/w06/notes/cms98.pdf
- [12] L. Van der Maaten and G. Hinton, "Visualizing data using t-sne." Journal of machine learning research, vol. 9, no. 11, 2008.
- [13] D. P. Kingma and M. Welling, "Auto-encoding variational bayes," 2014.
- [14] T. Dang, F. Mascarich, S. Khattak, C. Papachristos, and K. Alexis, "Graph-based path planning for autonomous robotic exploration in subterranean environments," in 2019 IEEE/RSJ International Conference on Intelligent Robots and Systems (IROS), 2019, pp. 3105–3112.
- [15] O. Kupervasser, H. Kutomanov, M. Mushaelov, and R. Yavich, "Using diffusion map for visual navigation of a ground robot," *Mathematics*, vol. 8, no. 12, 2020. [Online]. Available: https://www.mdpi.com/2227-7390/8/12/2175
- [16] Y. F. Chen, S.-Y. Liu, M. Liu, J. Miller, and J. How, "Motion planning with diffusion maps," 10 2016.
- [17] A. A. Hagberg, D. A. Schult, and P. J. Swart, "Exploring network structure, dynamics, and function using networkx," in *Proceedings of* the 7th Python in Science Conference, G. Varoquaux, T. Vaught, and J. Millman, Eds., Pasadena, CA USA, 2008, pp. 11 – 15.
- [18] P. Corke and J. Haviland, "Not your grandmother's toolbox the robotics toolbox reinvented for python," in 2021 IEEE International Conference on Robotics and Automation (ICRA), 2021, pp. 11357–11363.
- [19] A. Paszke, S. Gross, F. Massa, A. Lerer, J. Bradbury, G. Chanan, T. Killeen, Z. Lin, N. Gimelshein, L. Antiga, A. Desmaison, A. Kopf, E. Yang, Z. DeVito, M. Raison, A. Tejani, S. Chilamkurthy, B. Steiner, L. Fang, J. Bai, and S. Chintala, "Pytorch: An imperative style, high-performance deep learning library," in Advances in Neural Information Processing Systems 32, H. Wallach, H. Larochelle, A. Beygelzimer, F. d'Alché-Buc, E. Fox, and R. Garnett, Eds. Curran Associates, Inc., 2019, pp. 8024–8035. [Online]. Available: http://papers.neurips.cc/paper/9015-pytorch-an-imperative-style-high-performance-deep-learning-library.pdf
- [20] P. Cunningham and S. J. Delany, "k-Nearest Neighbour Classifiers: 2nd Edition (with Python examples)," arXiv e-prints, p. arXiv:2004.04523, Apr. 2020.